

## Article

# Physio-Biochemical Integrators and Transcriptome Analysis Reveal Nano-Elicitation Associated Response during *Dendrocalamus asper* (Schult. and Schult. F.) Backer ex K. Heyne Micropropagation

Anita Kumari <sup>1,2</sup> , Shubham Joshi <sup>1,2</sup> , Aqib Iqbal Dar <sup>1,2</sup> and Rohit Joshi <sup>1,2,\*</sup> 

<sup>1</sup> Division of Biotechnology, CSIR-Institute of Himalayan Bioresource Technology, Palampur 176061, India; anitakumarii.som@gmail.com (A.K.); shubham1431996@gmail.com (S.J.)

<sup>2</sup> Academy of Scientific and Innovative Research (AcSIR), Ghaziabad 201002, India

\* Correspondence: rohitjoshi@ihbt.res.in

**Abstract:** Bamboos are perennial, arborescent, monocarpic and industrially important non-timber plants. They are important for various purposes, such as carbon sequestration, biodiversity support, construction, and food and fiber production. However, traditional vegetative propagation is insufficient for bamboo multiplication. Moreover, little is known about the mechanism of gold nanoparticles (AuNPs) in vitro proliferation and regulation of physiological and biochemical properties. In this study, we investigated the impacts of citrate and cetyltrimethylammonium bromide (CTAB) coated AuNPs on in vitro proliferation, photosynthetic pigment content and antioxidant potential of *Dendrocalamus asper* (Schult. and Schult. F.) Backer ex K. Heyne. Various morpho-physiological and biochemical parameters were differentially affected along the citrate- and CTAB-coated AuNPs concentration gradients (200–600  $\mu\text{M}$ ). In vitro shoot proliferation, photosynthetic pigment content and antioxidant activities were higher in *D. asper* grown on Murashige and Skoog medium supplemented with 2  $\text{mg}\cdot\text{L}^{-1}$  benzyladenine and 400  $\mu\text{M}$  citrate-coated AuNPs than in those grown on Murashige and Skoog medium supplemented with 600  $\mu\text{M}$  CTAB-coated AuNPs. Identification of genes regulating in vitro *D. asper* proliferation will help understand the molecular regulation of AuNPs-mediated elicitation for modulating various physiological and biochemical activities during micropropagation. Gene Ontology enrichment analysis and Kyoto Encyclopedia of Genes and Genomes pathway analyses identified differentially expressed genes associated with in vitro modulation of AuNPs-regulated biological processes and molecular functions. The findings of this study provide new insight into AuNPs-mediated elicitation of in vitro mass scale bamboo propagation.

**Keywords:** bamboo; gold nanoparticles; RNA sequencing; tissue culture; transcriptome; transcription factors



**Citation:** Kumari, A.; Joshi, S.; Dar, A.I.; Joshi, R. Physio-Biochemical Integrators and Transcriptome Analysis Reveal Nano-Elicitation Associated Response during *Dendrocalamus asper* (Schult. and Schult. F.) Backer ex K. Heyne Micropropagation. *Genes* **2023**, *14*, 1725. <https://doi.org/10.3390/genes14091725>

Academic Editor: Jacqueline Batley

Received: 28 July 2023

Revised: 23 August 2023

Accepted: 25 August 2023

Published: 29 August 2023



**Copyright:** © 2023 by the authors. Licensee MDPI, Basel, Switzerland. This article is an open access article distributed under the terms and conditions of the Creative Commons Attribution (CC BY) license (<https://creativecommons.org/licenses/by/4.0/>).

## 1. Introduction

*Dendrocalamus asper* (Schult. & Schult. F.) Backer ex K. Heyne, also called giant bamboo or dragon bamboo, is a massive, tropical, sympodial bamboo species indigenous to Southeast Asia. Due to its large diameter of approximately 8–12 cm and 15–20 m tall straight culms, this bamboo has been utilized as a building material in heavy construction since time immemorial. Young *D. asper* shoots are sweet in taste and sold in canned or vacuum-packed packets [1]. Bamboo shoots can also be used to extract high-quality fiber for modern textile and clothing industries [2]. However, for continuous bamboo supply, new and sustainable propagation methods with reduced proliferation period are necessary to meet industrial demands. Thidiazuron (TDZ) supplemented Murashige and Skoog (MS) medium increases shoot proliferation of *D. asper* [3]. MS media supplemented with benzyladenine (BAP; 2  $\text{mg}\cdot\text{L}^{-1}$ ), kinetin (1  $\text{mg}\cdot\text{L}^{-1}$ ) and Naphthalene acetic acid (NAA;

0.5 mg·L<sup>-1</sup>) optimally induces callus formation and organogenesis [4]. Gonçalves et al., 2023 [5] reported that MS media supplemented with 2–3 mg·L<sup>-1</sup> BAP and 4 mg·L<sup>-1</sup> indole-3-butyric acid (IBA) resulted in shoot and root growth, respectively. Moreover, researchers have used various elicitors, including nano-particles (NPs) with various physical and chemical properties, to increase in vitro calli and shoot proliferation [6–12].

NPs are molecules or atomic aggregates ranging in size from 1 to 100 nm [6]. The concentration, size and physical characteristics of NPs affect plants in a species-specific and developmental stage-specific manner [7]. Engineered NPs have attracted much interest because of their prospects in increasing crop productivity. The progress in dedifferentiation, genetic transformation, biomass increment, reduced infection and proliferation of advantageous secondary metabolites have all benefited through nano-biotechnology [7]. Various nano-materials have been shown to penetrate the seed coat and improve water absorption and utilization by seeds [8]. Fe/SiO<sub>2</sub> nanomaterials have shown to enhance germination of barley and maize seeds [9]. Metal NPs have large surface areas and can exchange valance electrons with biomolecules more readily due to high surface area to volume ratio. Therefore, metal NPs can participate in cellular redox reactions and sugar biosynthesis pathways and change the antioxidant status of plants [10]. Gold nano-particles (AuNPs) comprise an inert core material to which surface coatings can be added, thereby functionalizing them and preventing the gold from interacting with the environment. Accumulation of AuNPs in plants can affect secondary metabolism and plant growth [11]. Emamverdian et al., 2020 [12] demonstrated that silver dioxide NPs increase bamboo plant biomass by enhancing its anti-oxidant potential under Pb stress. They further showed that 500 µM SiO<sub>2</sub> NPs effectively maintain plant growth under Pb toxicity.

De novo transcriptome analysis of *Phyllostachys edulis* identified genes involved in shoot elongation [13]. Thapa et al., 2022 [14] conducted a transcriptome study of in vitro *D. hamiltonii* plants to identify differentially expressed genes (DEGs) during juvenile and aged stages. However, the crucial regulatory genes involved in in vitro nano-elicitation in *D. asper* has not been studied yet. This study attempted to unravel the transcriptional programming that underlies nano-elicitation in *D. asper* plantlets grown in vitro. Transcriptomic analyses of genes underlying growth mechanisms may provide insight into key genes involved in growth, signaling and downstream activation of the oxidative stress tolerance mechanism [15]. This study revealed novel genes and their roles in enhancing *D. asper* growth and antioxidant potential. The complex signaling pathways underpinning oxidative stress-responsive signaling in *D. asper* are a functionally relevant and sustainable genomic resource for the advancement of genetic and metabolic engineering against oxidative stress.

Here we examined the effects of citrate- and cetyltrimethylammonium bromide (CTAB)-coated AuNPs on in vitro proliferation and antioxidant activities of the commercially important bamboo species i.e., *D. asper*. The objectives of this study were to: (1) identify the optimal citrate- and CTAB-coated AuNPs (citrate-AuNPs and CTAB-AuNPs) concentrations for stimulating *D. asper* shoot proliferation in vitro; (2) investigate the changes in physiological and biochemical properties of *D. asper* during in vitro nano-elicitation; and (3) assess the differential expression of genes through transcriptional profiling.

## 2. Materials and Methods

### 2.1. Plant Material, Treatment Conditions and Morphological Analysis

Aseptic in vitro cultures of *D. asper* were started from nodal explants in MS media containing BAP (2 mg·L<sup>-1</sup>) as described in previous study [5]. Previously synthesized and characterized citrate-AuNPs and CTAB-AuNPs were used in the present study [15]. MS media containing 3% sucrose, BAP and either citrate-AuNPs or CTAB-AuNPs at various concentrations, i.e., 200 µM, 400 µM and 600 µM, were prepared; pH was adjusted to 5.75–5.8 by adding either 1 M NaOH or HCl. Thereafter, 0.8% agar was added to the media. Nanoparticles were added post autoclaving, and Nps free MS medium supplemented with BAP was used as control. From one-month-old proliferated shoots, 8–10 culms were

excised and inoculated in MS media containing different concentrations of the NPs using sterile forceps in a laminar air flow chamber. Each treatment was performed in triplicate. The cultures were incubated at  $25 \pm 2$  °C under photoperiod of 16/8 h, light/dark for 30 days at a photosynthetic photon flux density of  $50 \text{ mmol}\cdot\text{m}^{-2}\cdot\text{s}^{-1}$  using white fluorescent LED tubes (20 W; Bajaj, Pune, India) and under 55–60% of relative humidity.

After 30 days, AuNPs treated *D. asper* micro-plantlets were picturized and shoot length was recorded. For each replicate, the number of shoots and leaves, as well as the overall plant biomass were recorded. The aggregate of plantlets from each treatment were collected, cleaned with sterile deionized water and dried among filter papers to calculate fresh weight (FW). Each replicate of control and treated cultures was oven-dried at 40 °C to determine the dry weight (DW).

### 2.2. Estimation of Total Chlorophyll, Soluble Sugar, Malondialdehyde Content, Phenolics Contents and Antioxidant Enzyme Assay

Chlorophyll a, chlorophyll b, total chlorophyll and total carotenoid contents were assessed, as previously described [16]. To quantify the photosynthetic pigment contents, absorbance was assessed with a UV-visible spectrophotometer at 663, 645 and 480 nm [15]. Total soluble sugar content was estimated using the anthrone method [17]. For each sample, total soluble sugar concentration was calculated using a glucose standard curve at 620 nm ( $y = 0.0376x + 0.0025$ ,  $R^2 = 0.9987$ ). Malondialdehyde (MDA) content was determined using the Heath and Packer, 1968 method [18]. Using a molar extinction coefficient of  $155 \text{ mM}^{-1}\cdot\text{cm}^{-1}$ , the MDA concentration was determined from absorbance at 532 nm. Total phenolics were isolated as defined earlier [19] and expressed as  $\text{mg}\cdot\text{g}^{-1}$  of the entire extract using the gallic acid standard curve ( $y = 0.0018x + 0.0048$ ,  $R^2 = 0.9986$ ). Further, AuNPs treated plantlets and their controls were homogenized in liquid nitrogen to measure superoxide dismutase (SOD) enzyme activity. The SOD enzymatic potential was determined by measuring absorbance at 560 nm, and 50% reduction in absorbance compared to that in the control was defined as one unit of enzyme activity [20].

### 2.3. RNA Isolation, Library Construction, Illumina Sequencing, Transcriptome Assembly and Annotation

Shoots grown in vitro on MS media containing 400  $\mu\text{M}$  of citrate-AuNPs or 600  $\mu\text{M}$  CTAB-AuNPs were used for further transcriptome analysis. Total RNA was isolated in triplicate using iRIS solution (CSIR-IHBT, Palampur, India) [21]. Spectrophotometric analysis and polyadenylate mRNA enrichment were performed, followed by cDNA library preparation, purified cDNA library quantification and paired end library preparation, as described earlier [14]. Paired end raw reads from Illumina Nova seq were pre-processed using the quality filtering tool, NGSQC tool kit v2.3 ([https://bioinformatics.home.com/tools/rna-seq/descriptions/NGS\\_QC\\_Toolkit.html#gsc.tab=0](https://bioinformatics.home.com/tools/rna-seq/descriptions/NGS_QC_Toolkit.html#gsc.tab=0); accessed on 15 November 2022) [22]. Base quality check of raw data was performed using FastQC (version 0.11.9; <https://www.bioinformatics.babraham.ac.uk/projects/fastqc/>; accessed on 30 November 2022). Illumina Adapter (AGATCGGAAGAGC) was removed using trim-galore (version 0.6.7; [https://software.cqls.oregonstate.edu/updates/trim\\_galore-0.6.7/](https://software.cqls.oregonstate.edu/updates/trim_galore-0.6.7/); accessed on 13 February 2023). HISAT2 v 2.4.0 (<http://daehwankimlab.github.io/hisat2/download/>; accessed on 18 March 2023) was used to assemble the reads from the samples. Mapped reads were assembled using Cufflinks (version 2.2.1; <http://cole-trapnell-lab.github.io/cufflinks/>; accessed on 25 April 2023) and the resulting transcripts were merged using Cuffmerge (<http://cole-trapnell-lab.github.io/cufflinks/cuffmerge/>; accessed on 3 May 2023) for use as reference to compare DEGs.

### 2.4. Differential Expression Analysis

After removing adapter sequences and low-quality reads, BAC (control), BAT1 (400  $\mu\text{M}$  citrate-treated) and BAT2 (600  $\mu\text{M}$  CTAB-treated) specific filter reads were mapped and assembled with reference to *D. latiflorus* genome, and the transcript abundance was estimated and normalized to fragments per kilobase of transcript per million mapped fragments

(FPKM) using the RNA-Seq by expectation-maximization (RSEM) tool [23]. EdgeR tool was used to detect differential expression of transcripts in treated plants compared with control plants, with a log fold change of 4.

The high-throughput sequencing data obtained through Cufflinks was screened for differentially expressed transcripts using the Cuffdiff tool. Significant DEGs were identified from the data; upregulated genes were defined by a  $\log_2FC \geq 4$  and corrected  $p$ -value  $\leq 0.05$ , while down-regulated genes were defined by a  $\log_2FC \leq -4$  and corrected  $p$ -value  $\leq 0.05$  (q-value). Identification of significant DEGs is more statistically stringent using reference-based assembly (*D. latiflorus*). CummeRbund was used for plotting. Annotation of the hits was performed using Uniprot database, Gene Ontology (GO) and Kyoto Encyclopedia Genes and Genomes (KEGG). MeV package v.4.9.0 was used to create heatmaps of DE transcripts based on FPKM values.

### 2.5. Functional Annotation and Pathway Analysis

Differentially regulated transcription factors in treated plants were predicted using the plant transcription factor database (PlantTFDB). Venn diagrams were plotted to interpret commonly and uniquely expressed genes among control; 400  $\mu$ M Citrate- and 600  $\mu$ M CTAB-treated plants. GO analysis of differentially expressed genes was performed using BLAST2Go. REduce and Visualize Gene Ontology (REVIGO) (<http://revigo.irb.hr/>) (accessed on 16 June 2023) visualization tool was used to summarize GO terms based on their semantic resemblances. Pathway analysis was performed by mapping the DEGs to the KEGG pathways database.

### 2.6. Statistical Analysis

SIGMA PLOT v 14.5 was used to perform all statistical analyses and create bar graphs. Each analysis was repeated three times in a completely randomized block design setup. Two-tailed Welch's  $t$ -test of  $p < 0.05$  was used to determine significance levels in each experiment and to compare the control and treated plants.

## 3. Results

### 3.1. Shoot Length and Total Biomass Increased in Plants Treated with Citrate and CTAB-AuNPs

Both citrate- and CTAB-AuNPs considerably improved biomass proliferation in a concentration-dependent manner (Figure 1). Each concentration of citrate- and CTAB-AuNPs significantly induced plant height, with the maximum plant height observed in plants treated with 400  $\mu$ M citrate-AuNPs (6.84 cm). The number of shoots in plants treated with citrate-AuNPs increased when the concentration was increased from 200  $\mu$ M (36) to 400  $\mu$ M (77.33); however, the number of shoots in plants treated with 600  $\mu$ M CTAB-AuNPs (25) also had significantly lesser number of shoots than control plants (31.66). Plants treated with 600  $\mu$ M CTAB-AuNPs (25) also had significantly lesser number of shoots than control plants. Increasing the concentration of citrate-AuNPs from 200  $\mu$ M to 400  $\mu$ M, significantly increased plant biomass (4.03 g to 8.4 g) compared to control (3.67 g). However, increasing CTAB-AuNPs concentration from 400  $\mu$ M to 600  $\mu$ M significantly reduced plant biomass from 2.35 g to 1.71 g (Figure 2).

### 3.2. Photosynthetic Pigment and Total Soluble Sugar Contents Increased after AuNPs-Treatment

Citrate- and CTAB-AuNPs differentially affected total chlorophyll pigment and soluble sugar contents in a concentration-dependent manner. Total chlorophyll and chlorophyll a and chlorophyll b contents in plants treated with 600  $\mu$ M citrate-AuNPs were significantly lower (3.89, 3.47, and 7.37  $\text{mg}\cdot\text{g}^{-1}$  fresh weight [FW], respectively) while those in plants treated with 400  $\mu$ M citrate-AuNPs were significantly higher (7.23, 3.99, and 11.22  $\text{mg}\cdot\text{g}^{-1}$  FW, respectively) than in control plants (4.99, 3.29, and 8.29  $\text{mg}\cdot\text{g}^{-1}$  FW, respectively). Treatment with 200  $\mu$ M CTAB-AuNPs also enhanced total chlorophyll and chlorophyll a and b contents (5.9, 5.44, and 11.35  $\text{mg}\cdot\text{g}^{-1}$  FW, respectively) significantly compared to those in controls (Figure 3A–C).

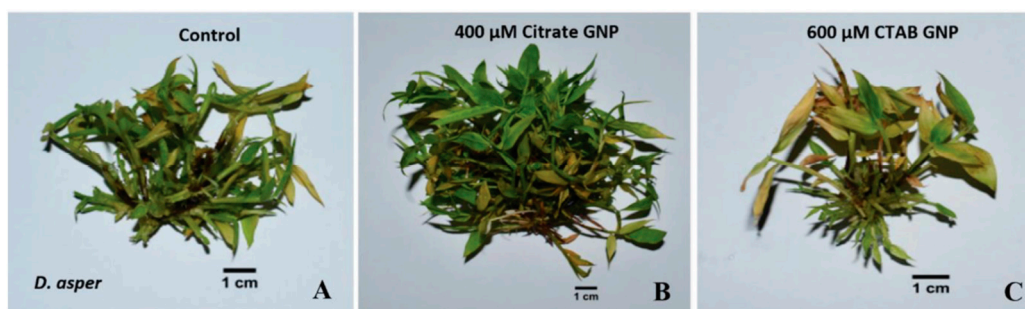


**Figure 1.** In vitro shoot proliferation and total biomass production in proliferated *D. asper* under control (MS + 2 mg·L<sup>-1</sup> BAP) and AuNP treated plants after 30 days. Biomass proliferation in (A) control; (B) 400 μM citrate-AuNP treated; and (C) 600 μM CTAB-AuNP treated. Scale bar = 1 cm.

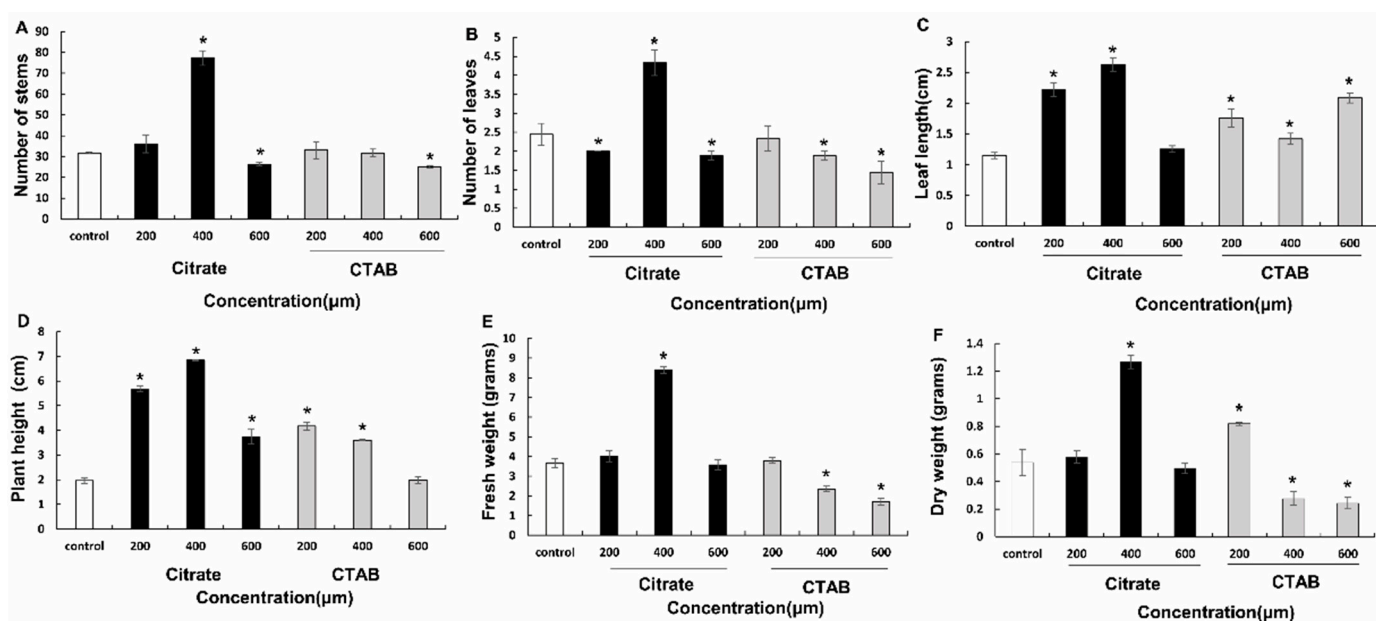


**Figure 2.** Effect of citrate and CTAB-AuNPs on growth and biomass enhancement of *D. asper*. (A) effect on number of stems; (B) effect on number of leaves; (C) effect on leaf length; (D) effect on plant height; (E) effect on fresh weight; and (F) effect on dry weight. The error bar represents standard error of three biological replicates. \* Indicates significantly reduced and enhanced parameters in comparison to the control.

Total soluble sugar level was significantly affected by both citrate- and CTAB-AuNPs in a concentration-dependent manner. As the concentration increased from 200 μM (1.83 mg·g<sup>-1</sup> FW) to 400 μM (2.40 mg·g<sup>-1</sup> FW), soluble sugar content increased significantly. In contrast, treatment with 600 μM citrate-AuNPs significantly reduced soluble sugar content in plants (1.55 mg·g<sup>-1</sup> FW). In plants treated with 600 μM CTAB-AuNPs, there were significant reductions in shoot number (25) and sugar content (1.084 mg·g<sup>-1</sup> FW), as shown in Figure 3D,E.

### 3.3. Total Phenolics, MDA and SOD Activity Increased after AuNPs Treatment

Phenolic content increased significantly in plants treated with 400 μM and 600 μM citrate- and CTAB-AuNPs. Maximum phenolic content was observed in plants treated with 600 μM citrate-AuNPs (0.25 mg·g<sup>-1</sup> DW). Similarly, SOD enzyme activity increased significantly in plants treated with citrate- and CTAB-AuNPs in a concentration-dependent manner. Plants treated with 600 μM CTAB-AuNPs (0.103 mg·g<sup>-1</sup> FW) showed the highest SOD activity. Moreover, MDA content increased significantly in plants treated with citrate- and CTAB-AuNPs in a concentration-dependent manner. The highest MDA content was

observed in plants treated with 600  $\mu\text{M}$  CTAB-AuNPs ( $0.027 \text{ mg}\cdot\text{g}^{-1}$  FW), as shown in Figure 4.

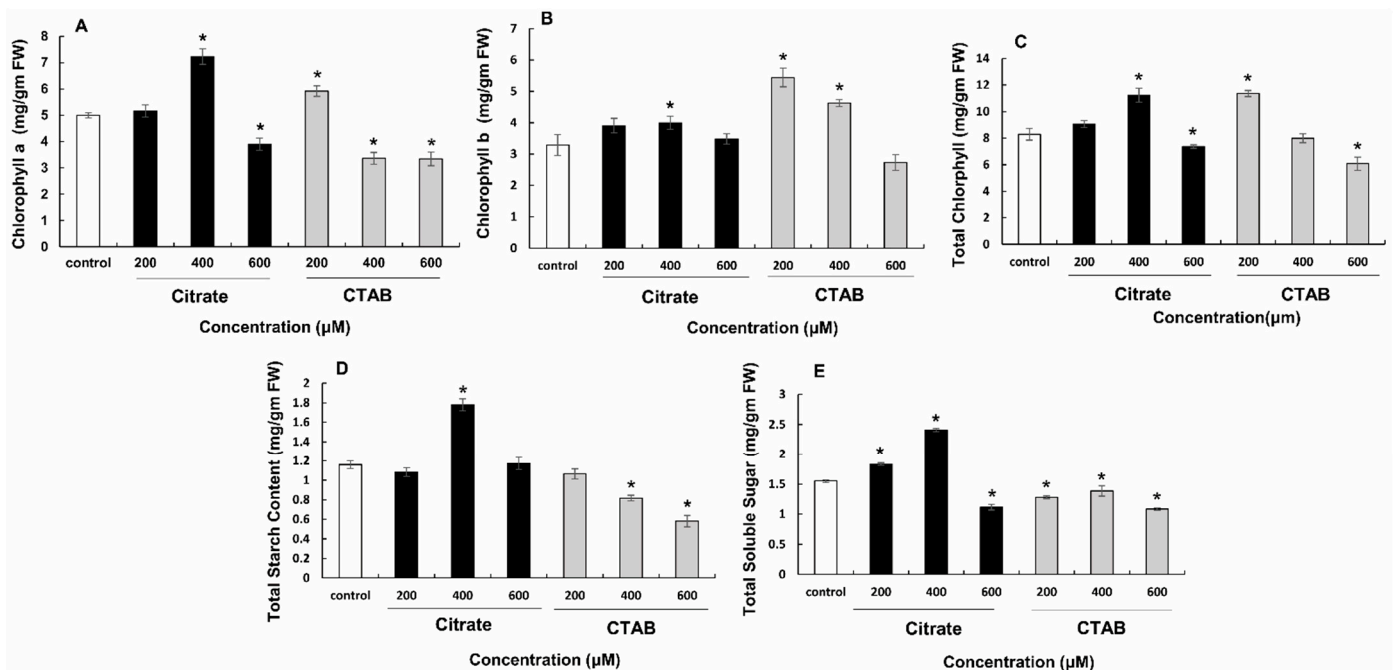


**Figure 3.** Effect of citrate and CTAB-AuNPs on photosynthetic pigments, sugar and starch content of *D. asper*. Effect on chlorophyll a (A), chlorophyll b (B) and total chlorophyll (C) content, respectively; (D) effect on total starch content; (E) effect on total soluble sugar content. The error bar represents the standard error of three biological replicates. \* Indicates significantly reduced and enhanced concentrations in comparison to the control.

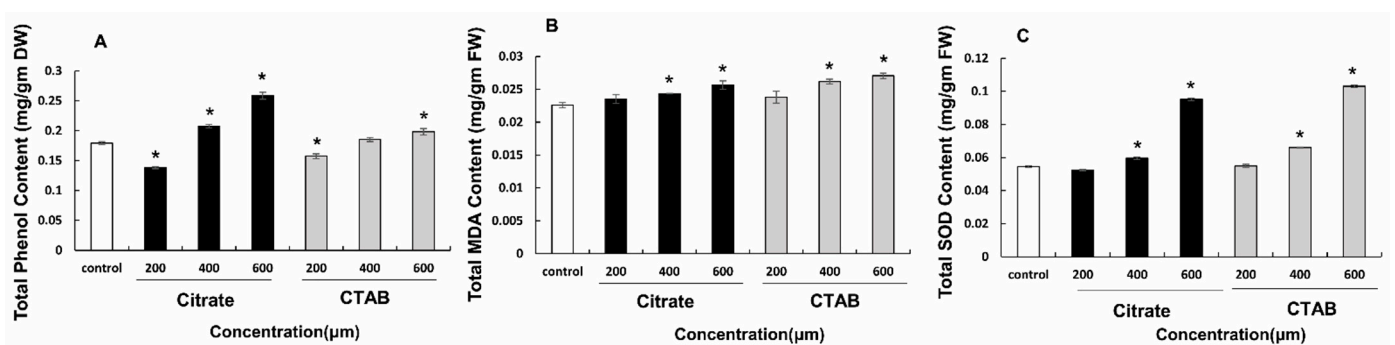


**Figure 4.** Effect of citrate and CTAB-AuNPs on antioxidant activity and lipid peroxidation of *D. asper*. (A) effect of total phenolic content; (B) effect of malondialdehyde content; and (C) effect on superoxide dismutase enzyme activity. The error bar represents standard error of three biological replicates. \* Indicates significantly reduced and enhanced concentrations in comparison to the control.

### 3.4. Transcriptome Analysis

To study the genes involved in biomass enhancement in *D. asper* due to nano-elicitation, RNA-seq analysis was performed on 30 days-old control and treated plants. Raw reads ranging from 3918968–26131133 produced by Illumina sequencing were analyzed (Supplementary Table S1). By filtering and eliminating adaptor sequences, high quality reads were obtained from raw reads using NGSQC toolkit v2.3; in total, 3670833–24406137 reads were obtained (Supplementary Table S2). The hits obtained for DEGs were annotated using UniProt via BLASTx (Supplementary Table S3; Figure 5).

S. No.	Condition	Total	On the basis of Differentially Expressed ( $\log_2FC \geq 2, \log_2FC \leq -2$ )		On the basis of Significant ( $q\text{-val} * 0.05$ )	On the basis of Differentially Expressed Significant ( $\log_2FC \geq 4, \leq -4$ and $q\text{-val} * 0.01$ )	
			↑	↓		↑	↓
1.	BAC vs BAT1	86,713	6,749	8,124	11,786	340	207
2.	BAC vs BAT2	86,713	9,839	5,597	12,420	640	156
3.	BAT2 vs BAT1	86,713	2,042	7,951	2,190	4	114

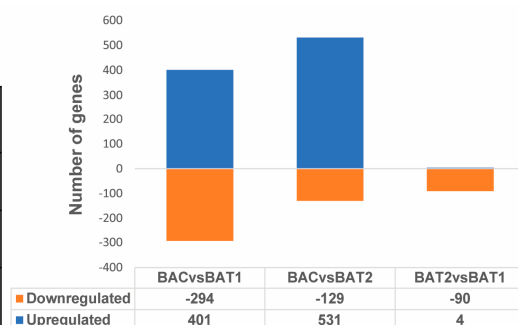


**Figure 5.** Differentially expressed genes in different treatment conditions in *D. asper*. \*  $q$ -value is a corrected  $p$ -value # Upregulated Genes- $\uparrow$ , Downregulated Genes- $\downarrow$ . BAC represents control, BAT1 represents 400  $\mu$ M citrate AuNPs and BAT2 represents 600  $\mu$ M CTAB AuNPs.

### 3.5. Differentially Expressed Genes after Nano-Elicitation

A total of 86,713 genes were identified; 401, 531 and 4 of these were significantly up-regulated in BAC vs. BAT1, BAC vs. BAT2 and BAT2 vs. BAT1 respectively, whereas 294, 129 and 90 were significantly down-regulated in BAC vs. BAT1, BAC vs. BAT2 and BAT2 vs. BAT1, respectively (Supplementary Tables S4 and S5). The Venn diagram representing significantly up-regulated and down-regulated genes between control and treated plants shows that 206 up-regulated and 90 down-regulated genes are common between BAC vs. BAT2 and BAC vs. BAT1, respectively (Figure 6). Similarly, 15 down-regulated genes were common between BAC vs. BAT1 and BAT2 vs. BAT1. Moreover, 66, 102 and 99 significantly down-regulated genes and 434, 134 and 4 significantly up-regulated genes were found in BAC vs. BAT2, BAC vs. BAT1 and BAT2 vs. BAT1, respectively. Additionally, the volcano plots show the distribution of significant DEGs (Figure 6A–C).

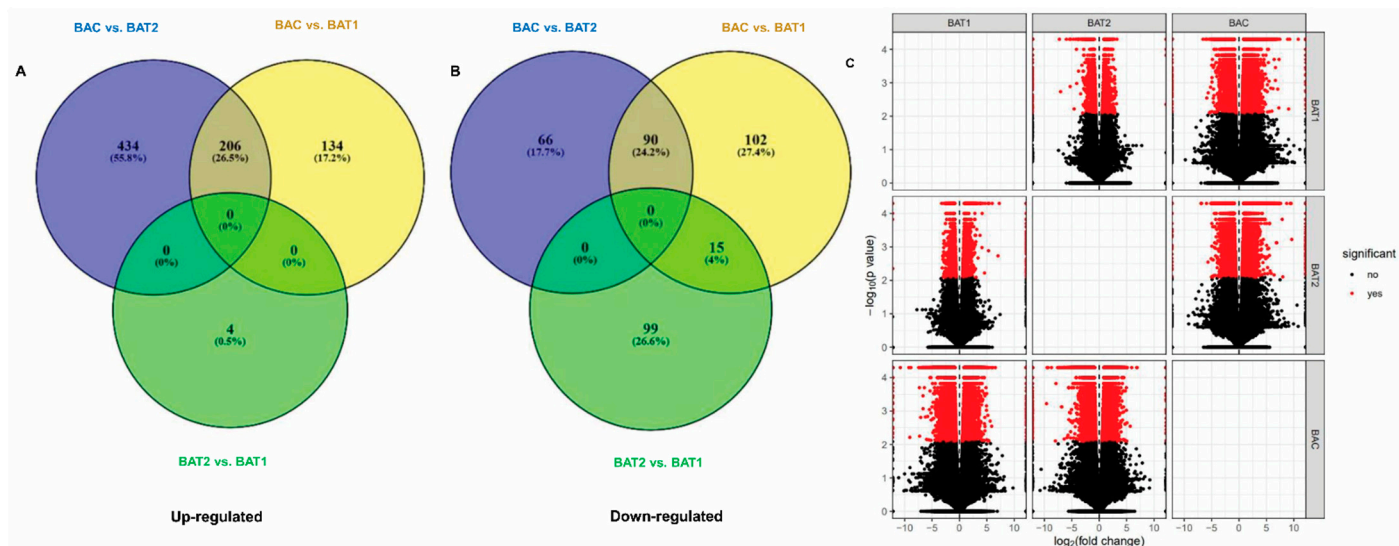


**Figure 6.** Venn diagram showing number of differentially expressed genes in different treatment conditions (400  $\mu$ M citrate vs. Control, 600  $\mu$ M CTAB vs. Control, 400  $\mu$ M citrate vs. 600  $\mu$ M CTAB) (A) Upregulated, (B) Downregulated genes. BAC represents control, BAT1 represents 400  $\mu$ M citrate AuNPs and BAT2 represents 600  $\mu$ M CTAB AuNPs. (C) Volcano plot showing the significant differentially expressed genes.

Furthermore, the heatmap scaled on  $\log_2$  fold change values shows the expression pattern of the top 50 differentially up-regulated and down-regulated genes. The heatmap showed the up-regulation of genes such as the auxin responsive protein IAA19 (XLOC\_067594), clathrin assembly protein (XLOC\_007685), histidine kinase 4 (XLOC\_053533), SNARE 13-like (XLOC\_016467), pyruvate kinase (XLOC\_005945) and WAT1-related protein (XLOC\_011969)

in BAT2 vs. BAT1, indicating their role in growth regulation, cell wall formation and anti-oxidant potential. The down-regulated genes in BAT2 vs. BAT1 were NAM protein (XLOC\_052155), glycosyl transferase (XLOC\_015241), E3 ubiquitin protein ligase (XLOC\_068769), MYB30 (XLOC\_061639) and calcium sensing receptor (XLOC\_040517). In BAC vs. BAT1, genes involved in cell wall synthesis and growth, such as cell wall protein gp-1-like (XLOC\_006413), aldehyde dehydrogenase (XLOC\_046769), phospholipase C (XLOC\_037233) and glucose-6-phosphate translocator2 (XLOC\_045665), were up-regulated. In contrast, the down-regulated genes were pathogenesis related protein (XLOC\_016574), WRKY70 TF (XLOC\_044267) and cytokinin oxidase (XLOC\_025307). Because WRKY 70 is involved in defense signaling pathway and cytokinin oxidase catalyses the degradation of cytokinin phytohormone, BAT1-treated plants showed better growth. Furthermore, in BAC vs. BAT2, up-regulation of senescence and phytohormone degradation related genes, such as cytokinin oxidase/dehydrogenase (XLOC\_007362), senescence specific cysteine protease (XLOC\_0025347), F-box protein (XLOC\_0242434), cysteine protease (XLOC\_018231) and anthocyanin reductase (XLOC\_023044), and down-regulation of aquaporin TIP4-1 (XLOC\_066291), metal transporter NRAT1 (XLOC\_040771), peroxidase P7-like (XLOC\_012240) and oxalate\_CoA ligase (XLOC\_061202) were observed (Figures 7 and 8). Besides these, 25 transcription factors were also differentially regulated, as shown in Figure 9.

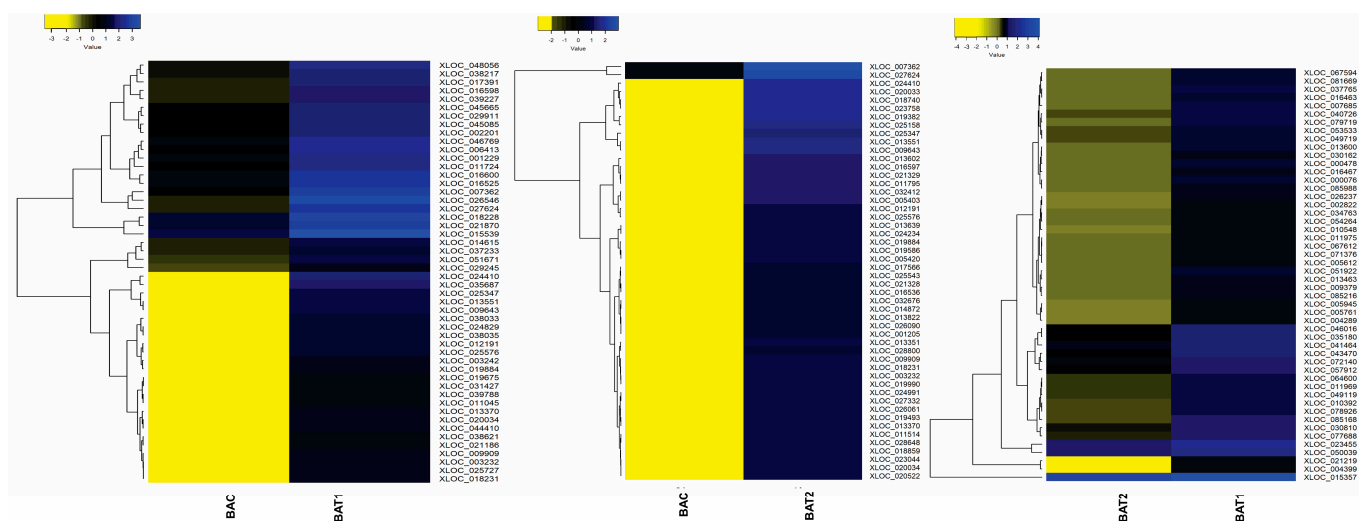


**Figure 7.** Heat maps showing differentially upregulated genes between control and AuNPs treated plants of *D. asper*. Heat map prepared at a log<sub>2</sub>fold scale of  $-4$  to  $+4$ . BAC represents control; BAT1 represents 400  $\mu$ M citrate AuNPs; and BAT2 represents 600  $\mu$ M CTAB AuNPs.

### 3.6. Functional Annotation and GO Analysis of Growth Responsive DEGs

GO analysis showed that growth responsive DEGs were enriched in molecular, cellular and biological processes. GO analysis was performed separately for up-regulated and down-regulated genes under each treatment condition, and significant annotation was represented as bar plots. The following biological functions were up-regulated in BAC vs. BAT1: extracellular stimulus, cold response, cell wall organization and response to light stimulus. The up-regulated biological processes in BAC vs. BAT2, were external and internal stimulus and abiotic stimulus, while those in BAT2 vs. BAT1 were cell wall biogenesis and cell growth. The down-regulated biological processes were transcription, RNA biosynthesis and response to organic substances in BAC vs. BAT1; transcription and response to organic substances in BAC vs. BAT2; and protein ubiquitination and protein conjugation in BAT2 vs. BAT1. The up-regulated molecular functions were 3-ketoacyl-CoA synthase activity, transporter activity and antiporter activity in BAC vs. BAT1; carboxylic acid, organic acid and amino acid transporter activities in BAC vs. BAT2; and 3-ketoacyl-CoA synthase activity and protein kinase activity in BAT2 vs. BAT1. The down-regulated molecular

functions were transcription factor activity and protein binding activity in BAC vs. BAT1 and BAC vs. BAT2, respectively, and GDP-fructose transmembrane transporter activity and transcription factor activity in BAT2 vs. BAT1. The up-regulated cellular components in BAC vs. BAT1 and BAC vs. BAT2 were plasma membrane, chloroplast and plastid, whereas those in BAT2 vs. BAT1 were cell wall, vesicle and Golgi apparatus 3-ketoacyl-CoA synthase activity and protein kinase activity. In contrast, the down-regulated cellular functions in BAC vs. BAT1, BAC vs. BAT2 and BAT2 vs. BAT1 were plasma membrane, nucleus and mitochondrion (Figure 10).

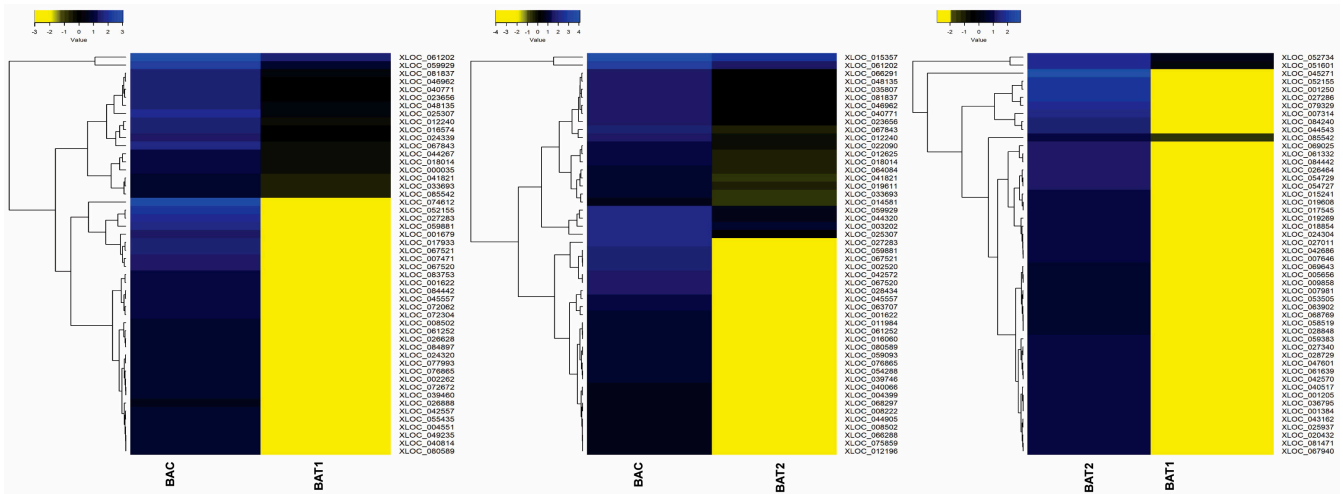


**Figure 8.** Differentially downregulated genes between control and AuNPs treated plants in *D. asper*. Heat map prepared at a log2fold scale of  $-4$  to  $+4$ . BAC represents control; BAT1 represents  $400 \mu\text{M}$  citrate AuNPs; and BAT2 represents  $600 \mu\text{M}$  CTAB AuNPs.

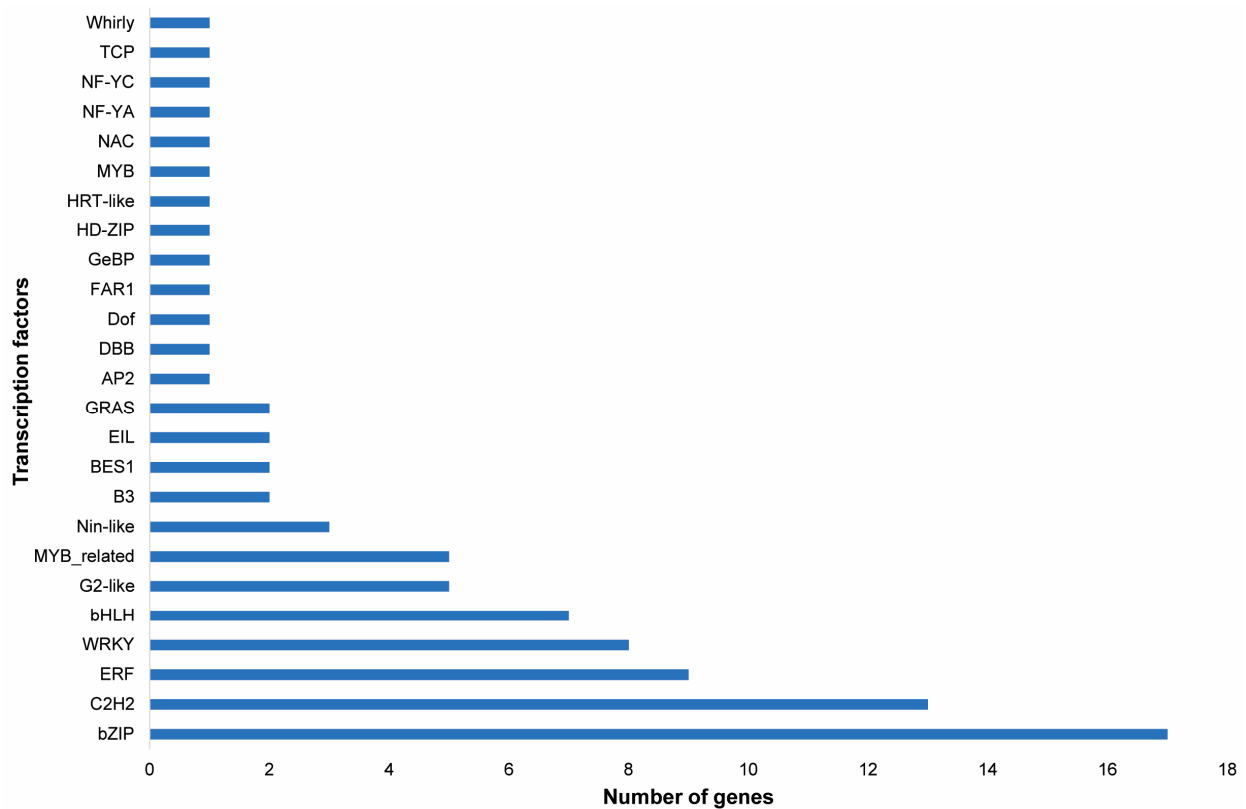


**Figure 9.** Differentially expressed transcription factors among control, citrate and CTAB coated gold nanoparticles.



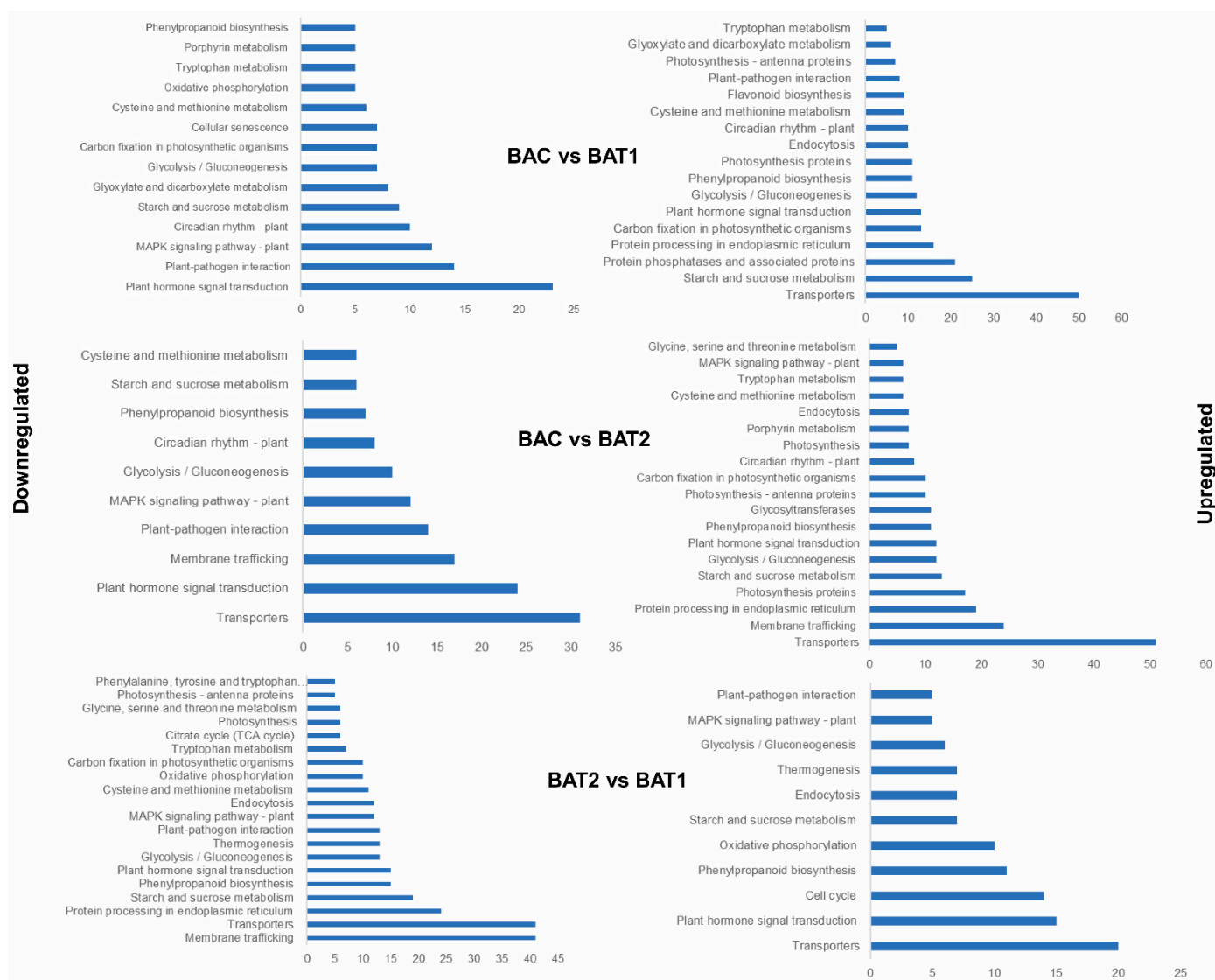


**Figure 11.** KEGG pathway analysis. KEGG enriched plant hormone signal transduction, transport, plant pathogen interaction and photosynthesis in BAC vs. BAT1, BAC vs. BAT2 and BAT2 vs. BAT1.

#### 4. Discussion

The use of NPs in agronomy and biotechnology for mass scale propagation and secondary metabolite production in different plants has increased significantly. Therefore, it is crucial to investigate how plants are affected by metallic and non-metallic NPs. AuNPs were previously found to be hazardous at concentrations  $\geq 100 \text{ mg} \cdot \text{L}^{-1}$  and particle diameter  $< 5 \text{ nm}$ ; however, their basic mechanism remains unclear. Under natural conditions, the chemistry of the coated material on NPs can change, altering the characteristics and stability of nanomaterials; however, surface alterations may stabilize them [15]. The growth of a species may be greatly influenced by the size and concentration of NPs. Surface coating is crucial for the stabilization of NPs, despite the risk of their aggregation in nutrient media. Positively or negatively charged coatings can affect how NPs interact with plasma membrane. Positively charged NPs assemble more readily on the cell surface than negatively charged ones because of electrostatic attraction. In contrast, negatively charged NPs can pass through the plasma membrane by forming potent covalent bonds [2]. The out-comes of the present study suggest that electrostatic repulsion may be overcome by smaller particles, regardless of charge, and that the difference in the metal ion gradient between, within and outside the cell may be a critical factor in internalization of NPs.

In this study, citrate-AuNPs and CTAB-AuNPs significantly boosted shoot proliferation, total biomass production, photosynthetic pigment content and anti-oxidant potential in bamboo in a dose-dependent manner [15]. Our study revealed that AuNPs boosted all growth parameters at optimum concentration but caused deterioration at higher concentrations. Despite being active, NPs at lower concentrations are not translocated to roots and shoots [24]. Previous studies showed that AgNPs cannot penetrate the roots at lower concentrations [25,26].

According to Acharya et al., 2019 [27], treatment with AuNPs boosted the overall light absorption by chlorophyll, accelerating the photochemical reaction and increasing the reducing power ( $\text{NADPH}^+$ ) and energy (ATP) available for  $\text{CO}_2$  fixation. The sugar content in treated plants approximately doubled, indicating better  $\text{CO}_2$  fixation [28]. Our study demonstrated that higher chlorophyll content increases  $\text{CO}_2$  fixation, increasing biomass produced per plant. Chlorophyll content is used to gauge a plant's capacity for photosynthetic activity affecting growth and development. Carotenoids absorb extra light and protect against photo-oxidation, which is harmful to the chlorophyll molecules [15]. In the present study, treatment with 400  $\mu\text{M}$  citrate-AuNPs and 200  $\mu\text{M}$  CTAB-AuNPs increased photosynthetic pigments. The up-regulation of reactive oxygen species (ROS)-scavenging enzymes may underlie this improvement in chlorophyll content in AuNPs-treated plants [29]. Total soluble sugars are essential for plant development, metabolism and maintenance of ROS balance in cells [30]. In our study, plants treated with 400  $\mu\text{M}$  citrate-AuNPs and 200  $\mu\text{M}$  CTAB-AuNPs had higher levels of total soluble sugar, indicating that the NPs positively influenced cellular metabolism, resulting in enhanced plant growth. Bananas grown in vitro have been shown to contain more chlorophyll and total soluble sugar when exposed to Ca-AuNPs and Ca-AuNP nano-composites coated with polyethylene glycol methacrylate [31].

MDA acts as a marker for oxidative stress, and plantlets supplemented with 400  $\mu\text{M}$  AuNPs showed accelerated growth and decreased MDA and proline contents due to enhanced anti-oxidant potential of enzymes. Plant biomass decreases at higher concentrations of AuNPs (600  $\mu\text{M}$ ) due to increased free radical formation, suggesting oxidative stress [32]. ROS are also involved in secondary metabolic pathways. The MDA level increased steadily with increase in citrate-AuNPs and CTAB-AuNPs concentrations. Nevertheless, the treated plantlets consistently accumulated lower MDA concentrations than the control plants, regardless of the AuNPs concentration. This clearly demonstrates that AuNPs may increase the effectiveness of electron exchange/transport reactions, thus reducing the oxidative load [33]. Phenolics have redox characteristics that enhance anti-oxidant potential of plants. By neutralizing the ROS produced during electron transport chain cycles, phenolic substances protect cells from oxidation [34]. The AuNPs used in this study increased total phenolic content in a concentration-dependent manner. NPs promote the generation of phenolics, increasing systemic acquired resistance [35].

The developmental switch regulating biomass/growth differences between control and treated plants is highly regulated by internal cues [36]. These regulatory components and mechanisms involved in sudden changes in the plant are not well-known. Thus, transcriptome analysis of control and treated *D. asper* micro-plantlets was performed to identify the genetic machinery regulating the visible changes in growth. In our transcriptome analysis, the filtered reads led to higher gene coverage, and high throughput sequencing using GO and KEGG showed the dominance of 'biological and metabolic processes, growth and stress related GO terms' in the biological category and 'plant hormone signal transduction, secondary metabolite and amino acid biosynthesis' in KEGG analysis are differentially regulated under control and treated conditions. This study identified growth responsive DEGs/transcripts involved in several biological, cellular and molecular processes.

The current study identified several transporters, including the V-type  $\text{H}^+$ -transporting ATPase subunit F, MFS transporter, ABC transporter 1, VGAT, Nrat1 and P-type  $\text{Ca}^{2+}$  transporter type 2C. These transporters handle various substances. The plasma membrane-localized Nrat1 has a broad substrate range including  $\text{Fe}^{2+}$ ,  $\text{Zn}^{2+}$ ,  $\text{Mn}^{2+}$ ,  $\text{Co}^{2+}$ ,  $\text{Cd}^{2+}$ ,  $\text{Cu}^{2+}$ ,

$\text{Ni}^{2+}$  and  $\text{Pb}^{2+}$ . NRAMP proteins are conserved and vital for metal ion balance. For instance, *AtNRAMP3* and *AtNRAMP4* in Arabidopsis transport iron from vacuoles to support plant growth [37]. Phospholipase C splits phosphatidylinositol 4,5-bisphosphate into DAG and IP<sub>3</sub>, acting as secondary messengers for cellular processes and other signaling molecule synthesis [38]. Similarly, the expression of clathrin assembly proteins increases when exposed to 400  $\mu\text{M}$  citrate, indicating increased metal ion intake. WAT1-related proteins, involved in secondary cell wall synthesis, also enhance in similar treatment. Our study confirms that anti-oxidant capacity and biomass accumulation are enhanced in plantlets treated with 400  $\mu\text{M}$  citrate.

This study revealed several significant DEGs that may be involved in mediating nano-elicited growth and anti-oxidant behavior of plants, including metal transporter *NRAT1*, cytokinin oxidase/dehydrogenase *CKX3* gene, PR-5, aquaporin TIP4-1, WRKY TF 70, peroxidase P7-like, NAC2 TF, aldehyde de-carboxylase, cell wall protein gp-1-like, isoamylase, phospholipase C, ferric reduction oxidase 7, glycosyltransferase, ABC transporter 1, E3 ubiquitin protein ligase, stromal cell-derived factor-2 like protein, IAA 19, SNARE-13-like, WAT1-related protein, ferritin-1, anthocyanin reductase and various transcription factors. These DEGs were involved in metal uptake, protein ubiquitination, cell wall synthesis, redox homeostasis, ethylene activated signaling and WRKY-regulated photomorphogenesis. AuNPs enter plantlets via basal shoot regions and are translocated by various metal transporters (*NRAT1* XLOC\_040771), leading to modulation of photomorphogenetic behavior and resulting in enhanced growth and anti-oxidant potential [39]. BAT1, i.e., 400  $\mu\text{M}$  citrate AuNPs, showed best biomass growth and enhanced anti-oxidant potential of bamboo. Cytokinin oxygenase/dehydrogenase (XLOC\_007362), isoamylase2 (XLOC\_014615) and phospholipase-C (XLOC\_037233) were up-regulated and may be linked to enhanced anti-oxidant activities. Moreover, MYBAS2 (XLOC\_029911), cell wall protein gp-1-like (XLOC\_006413) and proteins of photosystem 2 (XLOC\_002201), which were up-regulated, are involved in photosynthesis and growth processes. Thus, plantlets treated with 400  $\mu\text{M}$  citrate-AuNPs had better overall growth.

Transcription factors have a major role in modulating signaling pathways [40]. We identified differential expression of transcripts encoding *MYB*, *WRKY*, *DOF*, *GRAS*, *C2H2*, *TCP*, *B3*, *ERF*, *NAC*, *BES1* and *bZIP* TFs during growth and stress responses. These TFs are involved in the regulation of stomata opening and closing, anti-oxidant potential, cuticular wax biosynthesis, membrane modulation and cell wall biosynthesis [41]. Therefore, functional analysis of these genes to reveal their roles in modulating growth and oxidative behavior in bamboo might identify novel candidates to develop more resilient varieties.

## 5. Conclusions

The current study, for the first time, demonstrated that MS supplemented with BAP ( $2 \text{ mg} \cdot \text{L}^{-1}$ ) and 400  $\mu\text{M}$  citrate-AuNPs concentration increases anti-oxidant properties of bamboo species while also promoting shoot growth in a concentration-dependent manner. Citrate-AuNPs and CTAB-AuNPs enhanced anti-oxidant potential and synthesis of phenolic derivatives, thus reducing ROS production. Additionally, charged AuNPs can be used in tissue culture for quick and effective plant propagation as well as to reduce ROS production in bamboo species. Transcriptome analysis of in vitro regenerated shoots of control and treated plants has shown ways to find key regulators of growth changes in *D. asper*. It revealed various molecular and biological pathways modulated by various plant hormones and growth responsive genes after NP-treatment. Overall, our study provided significant insights into the transcriptome dynamics of nano-elicitation in bamboo. This study not only advances bamboo species propagation and applications but also basic research in genetic engineering and stress response.

**Supplementary Materials:** The following supporting information can be downloaded at: <https://www.mdpi.com/article/10.3390/genes14091725/s1>, Supplementary Table S1. Sequencing Data Report (Raw data); Supplementary Table S2. Sequencing Data Report (High Quality trimmed data); Supplementary Table S3. Blast X data; Supplementary Table S4. Raw data of significant differentially downregulated genes in BAC vs. BAT1, BAC vs. BAT2, respectively; Supplementary Table S5. Raw data of differentially downregulated genes in BAT2 vs. BAT1; Supplementary Table S6. Identification of genes regulating potential routes/pathways using KEGG database.

**Author Contributions:** A.K. performed the experiment, data collection and manuscript writing; S.J. participated in data analysis and manuscript writing; A.I.D. prepared the gold nanoparticles; R.J. conceived the idea, designed the study and reviewed and edited the final manuscript. All authors have read and agreed to the published version of the manuscript.

**Funding:** The financial support was provided by CSIR (MLP-201) and DBT (BT/PR45280/NER/95/1918/2022).

**Institutional Review Board Statement:** The study was approved by the Institutional Review Board. This manuscript represents CSIR-IHBT communication no. 5346.

**Informed Consent Statement:** Not applicable.

**Data Availability Statement:** The data are contained within the article and supplementary materials.

**Acknowledgments:** The authors thank the CSIR-Institute of Himalayan Bioresource Technology, Palampur, India, for support and for providing the infrastructure. Authors also thank Amitabha Acharya, CSIR-IHBT, Palampur, India for providing necessary facilities for nanoparticles preparation. A.K. and S.J. thank the UGC, GOI (NTA Ref. No.: 191620063807) and DBT, GOI (file No.: DBT/JRF/BET-19/1/2019/AL/212), respectively, for providing SRF.

**Conflicts of Interest:** The authors declare no conflict of interest. The funders had no role in the design of the study; in the collection, analyses or interpretation of data; in the writing of the manuscript; or in the decision to publish the results.

## References

1. Liese, W.; Köhl, M. *Bamboo. The Plant and Its Uses*; Springer: Cham, Switzerland, 2015. [CrossRef]
2. Sun, C.; Song, R.; Zhou, J.; Jia, Y.; Lu, J. Fermented bamboo fiber improves productive performance by regulating gut microbiota and inhibiting chronic inflammation of sows and piglets during late gestation and lactation. *Microbiol. Spectr.* **2023**, *11*, e04084-22. [CrossRef] [PubMed]
3. Gusmiaty, R.M.; Larekeng, S.H.; Setiawan, E. The optimization of in vitro micropropagation of betung bamboo (*Dendrocalamus asper* backer) by medium concentrations and plant growth regulators. *IOP Conf. Ser. Earth Environ. Sci.* **2020**, *575*, 12024. [CrossRef]
4. Zang, Q.; Liu, Q.; Zhuge, F.; Wang, X.; Lin, X. In vitro regeneration via callus induction in *Dendrocalamus asper* (Schult.) Backer. *Propag. Ornam. Plants* **2019**, *19*, 66–71. Available online: [http://www.journal-pop.org/2019\\_19\\_3\\_](http://www.journal-pop.org/2019_19_3_) (accessed on 16 June 2022).
5. Gonçalves, D.S.; Souza, D.M.S.C.; Molinari, L.V.; Avelar, M.L.M.; de Carvalho, D.; Teixeira, G.L.; Brondani, G.E. Clonal microplant production, morphological evaluation and genetic stability of *Dendrocalamus asper* (Schult. & Schult.) Backer ex. K. Heyneke. *Nativa* **2023**, *11*, 01–09. [CrossRef]
6. Karimi, J.; Mohsenzadeh, S. Effects of silicon oxide nanoparticles on growth and physiology of wheat seedlings. *Russ. J. Plant Physiol.* **2016**, *63*, 119–123. [CrossRef]
7. Emamverdian, A.; Ding, Y.; Mokhberdoran, F.; Ahmad, Z.; Xie, Y. The effect of silicon nanoparticles on the seed germination and seedling growth of moso bamboo (*Phyllostachys edulis*) under cadmium Stress. *Pol. J. Environ. Stud.* **2021**, *30*, 3033–3042. [CrossRef]
8. Banerjee, J.; Kole, C. Plant nanotechnology: An overview on concepts, strategies, and tools. In *Plant Nanotechnology*; Kole, C., Kumar, D., Khodakovskaya, M., Eds.; Springer: Cham, Switzerland, 2016; pp. 1–14. [CrossRef]
9. Najafi Disfani, M.; Mikhak, A.; Kassae, M.Z.; Maghari, A. Effects of nano Fe/SiO<sub>2</sub> fertilizers on germination and growth of barley and maize. *Arch. Agron. Soil Sci.* **2017**, *63*, 817–826. [CrossRef]
10. Alkhatib, R.; Alkhatib, B.; Abdo, N. Effect of Fe<sub>3</sub>O<sub>4</sub> nanoparticles on seed germination in tobacco. *Environ. Sci. Pollut. Res.* **2021**, *28*, 53568–53577. [CrossRef]
11. Kulus, D.; Tymoszek, A.; Jedrzejczyk, I.; Winiecki, J. Gold nanoparticles and electromagnetic irradiation in tissue culture systems of bleeding heart: Biochemical, physiological, and (cyto) genetic effects. *Plant Cell Tiss. Org. Cult.* **2022**, *149*, 715–734. [CrossRef]
12. Emamverdian, A.; Ding, Y.; Mokhberdoran, F.; Xie, Y.; Zheng, X.; Wang, Y. Silicon dioxide nanoparticles improve plant growth by enhancing antioxidant enzyme capacity in bamboo (*Pleuroblastus pygmaeus*) under lead toxicity. *Trees* **2020**, *36*, 469–481. [CrossRef]

13. Lan, Y.; Wu, L.; Wu, M.; Liu, H.; Gao, Y.; Zhang, K.; Xiang, Y. Transcriptome analysis reveals key genes regulating signaling and metabolic pathways during the growth of moso bamboo (*Phyllostachys edulis*) shoots. *Physiol. Plant.* **2021**, *172*, 91–105. [[CrossRef](#)] [[PubMed](#)]
14. Thapa, P.; Sareen, B.; Swarnkar, M.K.; Sood, A.; Bhattacharya, A. De novo transcriptome analysis of bamboo in vitro shoots for identification of genes differentiating juvenile and aged plants. *Ind. Crops. Prod.* **2022**, *176*, 114353. [[CrossRef](#)]
15. Joshi, S.; Dar, A.I.; Acharya, A.; Joshi, R. Charged Gold Nanoparticles Promote In Vitro Proliferation in *Nardostachys jatamansi* by Differentially Regulating Chlorophyll Content, Hormone Concentration, and Antioxidant Activity. *Antioxidants* **2022**, *11*, 1962. [[CrossRef](#)] [[PubMed](#)]
16. Arnon, D.I. Copper enzymes in isolated chloroplasts. Polyphenoloxidase in *Beta vulgaris*. *Plant Physiol.* **1949**, *24*, 1–15. [[CrossRef](#)] [[PubMed](#)]
17. Fazal, T.; Ismail, B.; Khan, A.M.; Khan, R.A.; Naqvi, A.A.S.; Hamid, F.S.; Sabir, M.A.; Faridullah Khan, A.R. Comparative studies on the use of binary and ternary combinations of various acidifying agents for the reduction of soil pH. *Commun. Soil Sci. Plant Anal.* **2016**, *47*, 11–18. [[CrossRef](#)]
18. Heath, R.L.; Packer, L. Photoperoxidation in isolated chloroplasts: I. Kinetics and stoichiometry of fatty acid peroxidation. *Arch. Biochem. Biophys.* **1968**, *125*, 189–198. [[CrossRef](#)]
19. Ahmed, A.F.; Attia, F.A.; Liu, Z.; Li, C.; Wei, J.; Kang, W. Antioxidant activity and total phenolic content of essential oils and extracts of sweet basil (*Ocimum basilicum* L.) plants. *Food Sci. Hum. Wellness.* **2019**, *8*, 299–305. [[CrossRef](#)]
20. Dhindsa, R.S.; Plumb-Dhindsa, P.A.; Thorpe, T.A. Leaf senescence: Correlated with increased levels of membrane permeability and lipid peroxidation, and decreased levels of superoxide dismutase and catalase. *J. Exp. Bot.* **1981**, *32*, 93–101. [[CrossRef](#)]
21. Ghawana, S.; Paul, A.; Kumar, H.; Kumar, A.; Singh, H.; Bhardwaj, P.K.; Rani, A.; Singh, R.S.; Raizada, J.; Singh, K.; et al. An RNA isolation system for plant tissues rich in secondary metabolites. *BMC Res. Notes* **2011**, *4*, 85. [[CrossRef](#)]
22. Patel, R.K.; Jain, M. NGS QC Toolkit: A toolkit for quality control of next generation sequencing data. *PLoS ONE* **2012**, *7*, e30619. [[CrossRef](#)]
23. Li, B.; Dewey, C.N. RSEM: Accurate transcript quantification from RNA-Seq data with or without a reference genome. *BMC Bioinform.* **2011**, *12*, 323. [[CrossRef](#)] [[PubMed](#)]
24. Milewska-Hendel, A.; Gepfert, W.; Zubko, M.; Kurczyńska, E. Morphological, Histological and Ultrastructural Changes in *Hordeum vulgare* (L.) Roots That Have Been Exposed to Negatively Charged Gold Nanoparticles. *Appl. Sci.* **2022**, *12*, 3265. [[CrossRef](#)]
25. Mahakham, W.; Theerakulpisut, P.; Maensiri, S.; Phumying, S.; Sarmah, A.K. Environmentally benign synthesis of phytochemicals-capped gold nanoparticles as nanoprimer agent for promoting maize seed germination. *Sci. Total Environ.* **2016**, *573*, 1089–1102. [[CrossRef](#)]
26. Rastogi, A.; Zivcak, M.; Sytar, O.; Kalaji, H.M.; He, X.; Mbarki, S.; Brestic, M. Impact of Metal and Metal Oxide Nanoparticles on Plant: A Critical Review. *Front Chem.* **2017**, *5*, 78. [[CrossRef](#)] [[PubMed](#)]
27. Acharya, P.; Jayaprakasha, G.K.; Crosby, K.M.; Jifon, J.L.; Patil, B.S. Green-synthesized nanoparticles enhanced seedling growth, yield, and quality of onion (*Allium cepa* L.). *ACS Sustain. Chem. Eng.* **2019**, *7*, 14580–14590. [[CrossRef](#)]
28. Venzhik, Y.; Deryabin, A.; Popov, V.; Dykman, L.; Moshkov, I. Priming with gold nanoparticles leads to changes in the photosynthetic apparatus and improves the cold tolerance of wheat. *Plant Physiol. Biochem.* **2022**, *190*, 145–155. [[CrossRef](#)] [[PubMed](#)]
29. Singh, A.; Mehta, S.; Yadav, S.; Nagar, G.; Ghosh, R.; Roy, A.; Chakraborty, A.; Singh, I.K. How to cope with the challenges of environmental stresses in the era of global climate change: An update on ROS stress in plants. *Int. J. Mol. Sci.* **2022**, *23*, 1995. [[CrossRef](#)]
30. Wang, Q.; Hu, J.; Lou, T.; Li, Y.; Shi, Y.; Hu, H. Integrated agronomic, physiological, microstructure, and whole-transcriptome analyses reveal the role of biomass accumulation and quality formation during Se biofortification in alfalfa. *Front. Plant Sci.* **2023**, *14*, 1198847. [[CrossRef](#)]
31. Anwar, N.; Wahid, J.; Uddin, J.; Khan, A.; Shah, M.; Shah, S.A.; Subhan, F.; Khan, M.A.; Ali, K.; Rauf, M.; et al. Phytosynthesis of poly (ethylene glycol) methacrylate-hybridized gold nanoparticles from *C. tuberculata*: Their structural characterization and potential for in vitro growth in banana. *Vitr. Cell. Dev. Biol.* **2021**, *57*, 248–260. [[CrossRef](#)]
32. Farooq, M.A.; Niazi, A.K.; Akhtar, J.; Farooq, M.; Souri, Z.; Karimi, N.; Rengel, Z. Acquiring control: The evolution of ROS-Induced oxidative stress and redox signaling pathways in plant stress responses. *Plant Physiol. Biochem.* **2019**, *141*, 353–369. [[CrossRef](#)]
33. Golinejad, S.; Mirjalili, M.H.; Rezaeost, H.; Ghorbanpour, M. Molecular, biochemical, and metabolic changes induced by gold nanoparticles in *Taxus baccata* L. cell culture. *Ind. Crops Prod.* **2023**, *192*, 115988. [[CrossRef](#)]
34. Shen, Y.; Guan, Y.; Song, X.; He, J.; Xie, Z.; Zhang, Y.; Zhang, H.; Tang, D. Polyphenols extract from lotus seedpod (*Nelumbo nucifera* Gaertn.): Phenolic compositions, antioxidant, and antiproliferative activities. *Food Sci. Nutr.* **2019**, *7*, 3062–3070. [[CrossRef](#)] [[PubMed](#)]
35. Afzal, S.; Aftab, T.; Singh, N.K. Impact of zinc oxide and iron oxide nanoparticles on uptake, translocation, and physiological effects in *Oryza sativa* L. *J. Plant Growth Regul.* **2022**, *41*, 1445–1461. [[CrossRef](#)]
36. Joshi, S.; Chinnusamy, V.; Joshi, R. Root System Architecture and Omics Approaches for Belowground Abiotic Stress Tolerance in Plants. *Agriculture* **2022**, *12*, 1677. [[CrossRef](#)]

37. Zhu, B.; Gan, C.; Gu, L.; Du, X.; Wang, H. Identification of *NRAMP4* from *Arabis paniculata* enhance cadmium tolerance in transgenic *Arabidopsis*. *J. Genet.* **2021**, *100*, 89. [[CrossRef](#)]
38. Suh, P.G.; Park, J.I.; Manzoli, L.; Cocco, L.I.; Peak, J.C.; Katan, M.; Fukami, K.; Kataoka, T.; Yun, S.; Ryu, S.H. Multiple roles of phosphoinositide-specific phospholipase C isozymes. *BMB Rep.* **2008**, *41*, 415–434. [[CrossRef](#)]
39. Roychoudhury, A. (Ed.) *Biology and Biotechnology of Environmental Stress Tolerance in Plants: Volume 2: Trace Elements in Environmental Stress Tolerance*; CRC Press: Boca Raton, FL, USA, 2023.
40. Wani, S.H.; Anand, S.; Singh, B.; Bohra, A.; Joshi, R. WRKY transcription factors and plant defense responses: Latest discoveries and future prospects. *Plant Cell Rep.* **2021**, *40*, 1071–1085. [[CrossRef](#)] [[PubMed](#)]
41. Joshi, R.; Wani, S.H.; Singh, B.; Bohra, A.; Dar, Z.A.; Lone, A.A.; Pareek, A.; Singla-Pareek, S.L. Transcription factors and plants response to drought stress: Current understanding and future directions. *Front. Plant Sci.* **2016**, *7*, 1029. [[CrossRef](#)] [[PubMed](#)]

**Disclaimer/Publisher's Note:** The statements, opinions and data contained in all publications are solely those of the individual author(s) and contributor(s) and not of MDPI and/or the editor(s). MDPI and/or the editor(s) disclaim responsibility for any injury to people or property resulting from any ideas, methods, instructions or products referred to in the content.